Theory of Anisotropic Diffusion of Entangled and Unentangled Polymers in Rod-Sphere Mixtures: Supplemental Materials

Umi Yamamoto[1,#] and Kenneth S. Schweizer[2,3*]

Department of Physics[1], Departments of Materials Science and Chemistry[2], and Frederick Seitz Materials Research Laboratory[3], University of Illinois, Urbana, IL 61801

*kschweiz@illinois.edu

#present address: Division of Chemistry and Chemical Engineering, California Institute of Technology, Pasadena, CA

Section A presents mathematical details of the theory and analytic derivations that underlie the results discussed in the main text. Section B presents an analytic analysis and numerical results for the needle localization transition, including physical discussion and interpretation.

A. Mathematical Derivations

We briefly summarize the derivation of Eqs. (3a) and (3b) and a few analytic relations given in the main text. The derivation of Eq. (1) is sketched in Ref. [1] and will be discussed in depth in a future article. A general approach to solve Eq. (1) is to find a vector function such that

$$\Omega_e^{(r\alpha)\dagger}\vec{f}^{(r\alpha)}(\vec{r}) = \left[\left(\vec{\nabla}+\vec{T}^{(r\alpha)}\right)\cdot\left(\hat{D}^{(r)}+\hat{D}^{(\alpha)}\right)\cdot\vec{\nabla}\right]\vec{f}^{(r\alpha)}(\vec{r}) = \vec{T}^{(r\alpha)}(\vec{r}), \qquad \text{(A1)}$$

so the inverse operator in Eq. (1) can be replaced by substituting $\left[\Omega_e^{(r\alpha)\dagger}\right]^{-1}\vec{T}^{(r\alpha)}(\vec{r}) = \vec{f}^{(r\alpha)}(\vec{r})$. The rod-rod component was discussed and derived in Ref. [2], while the rod-sphere component is most conveniently expressed in a cylindrical coordinate system where the origin is at the tagged rod center-of-mass and the z-axis is aligned with rod orientation. The rod-sphere T-operator, $\vec{T}^{(rs)}(\vec{r})$, is formally derived as the derivative of the non-overlapping condition between a rod and a sphere as introduced in Ref. [1]. Each vector function is expressed as $\vec{T}^{(rs)}(\vec{r}) = \hat{\rho}^{'}T_\rho(\vec{r}^{'}) + \hat{z}^{'}T_z(\vec{r}^{'})$ and $\vec{f}^{(rs)}(\vec{r}^{'}) = \hat{\rho}^{'} f_\rho^{(rs)}(\vec{r}^{'}) + \hat{z}^{'} f_z^{(rs)}(\vec{r}^{'})$, and one can express the components of $\vec{T}^{(rs)}(\vec{r})$ as

$$T_\rho \equiv \frac{1}{R}\Theta\left(\gamma\varepsilon - |z^{'}|\right)\delta(\rho^{'}-1) + \frac{1}{R}\rho^{'}\Theta\left(|z^{'}|-\gamma\varepsilon\right)\delta\left(\sqrt{\rho^{'2}+(|z^{'}|-\gamma\varepsilon)^2}-1\right), \qquad \text{(A2a)}$$

$$T_z \equiv \frac{z^{'}}{|z^{'}|}\frac{1}{\varepsilon R}\left(|z^{'}|-\gamma\varepsilon\right)\Theta\left(|z^{'}|-\gamma\varepsilon\right)\delta\left(\sqrt{\rho^{'2}+(|z^{'}|-\gamma\varepsilon)^2}-1\right), \qquad \text{(A2b)}$$

where the ρ and z axes are re-scaled as $\rho^{'} \equiv \rho / R$ and $z^{'} \equiv \varepsilon z / R$, and $\varepsilon \equiv \sqrt{D_{\perp}^{(r)} / D_{\parallel}^{(r)}}$. Substituting Eq. (A2) in Eq. (1), one obtains a Laplace equation from its regular part, $\nabla^{'2} \vec{f}^{(rs)}(\vec{r}^{'}) = 0$, and the following boundary condition from the singular part:

$$\left[\rho^{'}\partial_{\rho}^{'} + \frac{z^{'}}{|z^{'}|}\left(\frac{|z^{'}|-\gamma\varepsilon}{\varepsilon^{2}}\right)\Theta\left(|z^{'}|-\gamma\varepsilon\right)\partial_{z^{'}}\right] f_{\rho}^{(rs)}\Big|_{\partial\Omega^{'}} = \frac{R}{D_{\perp}^{(r)}}\left[\rho^{'}\Theta\left(|z^{'}|-\gamma\varepsilon\right) + \Theta\left(\gamma\varepsilon - |z^{'}|\right)\right], \quad \text{(A3a)}$$

$$\left[\rho^{'}\partial_{\rho}^{'} + \frac{z^{'}}{|z^{'}|}\left(\frac{|z^{'}|-\gamma\varepsilon}{\varepsilon^{2}}\right)\Theta\left(|z^{'}|-\gamma\varepsilon\right)\partial_{z^{'}}\right] f_{z}^{(rs)}\Big|_{\partial\Omega^{'}} = \frac{R}{\varepsilon D_{\perp}^{(r)}}\frac{z^{'}}{|z^{'}|}(|z^{'}|-\gamma\varepsilon)\Theta\left(|z^{'}|-\gamma\varepsilon\right), \quad \text{(A3b)}$$

where the boundary $\partial\Omega^{'}$ corresponds to a "distorted" spherocylinder of length $\gamma\varepsilon$ and oblate spheroidal caps of unit equatorial radius and polar radius ε. While the left-hand side of Eqs. (A3a) and (A3b) formally involve two derivatives, they in fact represent normal derivatives to the boundary on both the cylindrical and spheroidal domains; the former is trivial, and the latter can be verified for each cap by shifting the $z^{'}$-axis via $z^{'} \to z^{'} \pm \gamma\varepsilon$ and changing to an appropriate spheroidal coordinate. However, obtaining a closed analytic form is not possible without an approximation for the boundary shape. Thus, we replace the distorted spherocylinder by a spheroid with the same aspect ratio, $(1+\gamma)\varepsilon$. The appropriate orthogonal coordinate for this boundary is the prolate (or oblate, when applicable) spheroidal coordinate, defined via

$$\rho^{'} = a\sqrt{\zeta^{2}-1}\sqrt{1-\mu^{2}}, \quad z^{'} = a\zeta\mu, \quad \varphi = \tan^{-1}(y^{'}/x^{'}), \quad a \equiv \sqrt{(1+\gamma)^{2}\varepsilon^{2}-1}, \quad \text{(A4)}$$

where $1 \le \zeta < \infty$, $-1 \le \mu \le 1$, and $\zeta = \zeta_{0} \equiv (1+\gamma)\varepsilon / \sqrt{|(1+\gamma)^{2}\varepsilon^{2}-1|}$ now represents the boundary. Equation (A4) applies only if $\varepsilon = \sqrt{D_{\perp}^{(r)} / D_{\parallel}^{(r)}} > 1/(1+\gamma)$, otherwise an equivalent oblate spheroidal coordinate is required. In the former case, the Laplace equation is given by

$$\left\{\frac{1}{a^2(\zeta^2-\mu^2)}\left[\partial_\zeta(\zeta^2-1)\partial_\zeta+\partial_\mu(1-\mu^2)\partial_\mu\right]+\frac{1}{a^2(\zeta^2-1)(1-\mu^2)}\partial_\varphi^2\right\}\vec{f}^{(rs)}(\zeta,\mu)=0, \quad \text{(A5)}$$

whereas the boundary conditions can be expressed as

$$\left(\frac{\zeta_0^2-1}{\zeta_0}\right)\partial_\zeta f_\rho^{(rs)}(\zeta,\mu)\bigg|_{\zeta=\zeta_0}=\frac{R}{D_\perp^{(r)}}\left[\sqrt{1-\mu^2}\,\Theta\left(|\mu|-\frac{\gamma}{1+\gamma}\right)+\Theta\left(\frac{\gamma}{1+\gamma}-|\mu|\right)\right], \quad \text{(A6a)}$$

$$\left(\frac{\zeta_0^2-1}{\zeta_0}\right)\partial_\zeta f_z^{(rs)}(\zeta,\mu)\bigg|_{\zeta=\zeta_0}=\frac{R(1+\gamma)}{D_\perp^{(r)}}\frac{\mu}{|\mu|}\left(|\mu|-\frac{\gamma}{1+\gamma}\right)\Theta\left(|\mu|-\frac{\gamma}{1+\gamma}\right). \quad \text{(A6b)}$$

Note that we used the following form for the gradient:

$$\vec{\nabla}'=\hat{\rho}'\,\frac{\sqrt{(\zeta^2-1)(1-\mu^2)}}{a(\zeta^2-\mu^2)}(\zeta\partial_\zeta-\mu\partial_\mu)+\hat{z}'\,\frac{1}{a(\zeta^2-\mu^2)}\left[\mu(\zeta^2-1)\partial_\zeta+\zeta(1-\mu^2)\partial_\mu\right]. \quad \text{(A7)}$$

For the oblate coordinate system, one simply replaces ζ^2-1 and $\zeta^2-\mu^2$ with ζ^2+1 and $\zeta^2+\mu^2$, respectively, in Eqs. (A5), (A6) and (A7).

A general solution to Eqn. (A5) is obtained via separation of variables, and the one that is axially symmetric and convergent at $\zeta\to\infty$ is given by

$$f_i^{(rs)}(\zeta,\mu)=\sum_{n=0}^{\infty}A_n q_n(\zeta)P_n(\mu), \qquad (i=\rho, z) \quad \text{(A8)}$$

where $P_n(\mu)$ is the Legendre polynomial of the first kind, and $q_n(\zeta)$ is essentially the Legendre function of the second kind, defined via[3]

$$q_n(x)\equiv\frac{1}{2}P_n(x)\log\left(\frac{x+1}{x-1}\right)-\sum_{m=0}^{2m+1<n}\frac{2(n-m)-(2m+1)}{(2m+1)(n-m)}P_{n-(2m+1)}(x). \quad \text{(A9)}$$

Note $q_n(x)$ is replaced by $i^{(n+1)}q_n(ix)$ for the oblate spheroidal coordinate. The coefficients A_n are determined by substituting Eq. (A8) into Eqs. (A6a) and (A6b) and using the orthogonality relation for the Legendre polynomials, $\int_0^1 d\mu P_n(\mu)P_m(\mu) = 1/(2n+1)\delta_{nm}$. Then we find

$$f_\rho^{(rs)}(\zeta,\mu) = \frac{R}{D_\perp^{(r)}}\left(\frac{\zeta_0}{\zeta_0^2 \mp 1}\right)\sum_{n=0}^{\infty}\frac{(4n+1)}{q'_{2n}(\zeta_0)}c_{2n}\left(\frac{\gamma}{1+\gamma}\right)q_{2n}(\zeta)P_{2n}(\mu), \tag{A10a}$$

$$f_z^{(rs)}(\zeta,\mu) = \frac{R(1+\gamma)}{D_\perp^{(r)}}\left(\frac{\zeta_0}{\zeta_0^2 \mp 1}\right)\sum_{n=0}^{\infty}\frac{(4n+3)}{q'_{2n+1}(\zeta_0)}c_{2n+1}\left(\frac{\gamma}{1+\gamma}\right)q_{2n+1}(\zeta)P_{2n+1}(\mu), \tag{A10b}$$

where $c_n(x)$ is defined in the main text, and the minus or plus symbol corresponds to the prolate [$\varepsilon(1+\gamma)>1$] and oblate [$\varepsilon(1+\gamma)<1$] coordinate system, respectively.

The final results for Eq. (2) and (3) in the main text are obtained by substituting $\left[\Omega_e^{(r\alpha)\dagger}\right]^{-1}\vec{T}^{(r\alpha)}(\vec{r}) = \vec{f}^{(r\alpha)}(\vec{r})$ into Eq. (1) and taking the tensor contraction of Eq. (1) with $(1-\vec{u}_1\vec{u}_1^T)/2$ and $\vec{u}_1\vec{u}_1^T$:

$$\frac{1}{D_\perp^{(r)}} = \frac{1}{D_{\perp,0}^{(r)}} - \frac{(1-\vec{u}_1\vec{u}_1^T)}{2} : \sum_{\alpha=r,s}\rho_\alpha\int d\vec{r}\; g_{rs}(\vec{r})\vec{T}^{(r\alpha)}(\vec{r})\,\vec{f}^{(r\alpha)T}(\vec{r}), \tag{A11a}$$

$$\frac{1}{D_\parallel^{(r)}} = \frac{1}{D_{\parallel,0}^{(r)}} - (\vec{u}_1\vec{u}_1^T) : \sum_{\alpha=r,s}\rho_\alpha\int d\vec{r}\; g_{rs}(\vec{r})\vec{T}^{(r\alpha)}(\vec{r})\,\vec{f}^{(r\alpha)T}(\vec{r}), \tag{A11b}$$

Re-organizing Eqs. (A11a) and (A11b) yields Eq. (2). Note, for the rod-sphere term, the tensor contraction can be done in cylindrical coordinates where $(1-\vec{u}_1\vec{u}_1^T)/2 = (1-\hat{z}'\hat{z}'^T)/2$ and $\vec{u}_1\vec{u}_1^T = \hat{z}'\hat{z}'^T$, while the integral is easily manipulated in the spheroidal coordinate. To do so, one expresses the pair correlation function as $g_{rs}(\vec{r}) = \Theta(\zeta-\zeta_0)$ and the T-operator as:

$$\vec{T}^{(rs)}(\vec{r}) = \hat{\rho}\,\frac{\zeta_0\sqrt{\zeta_0^2 \mp 1}\sqrt{1-\mu^2}}{aR(\zeta_0^2 \mp \mu^2)}\,\delta(\zeta-\zeta_0) + \hat{z}\,\frac{\mu(\zeta_0^2 \mp 1)}{aR(\zeta_0^2 \mp \mu^2)}\,\delta(\zeta-\zeta_0)\,, \qquad \text{(A12)}$$

where we follow the sign convention discussed above. Finally, substituting Eqs. (A10a), (A10b) and (A12) into Eqs. (A11a) and (A11b) yields

$$\frac{1}{D_{\perp}^{(r)}} = \frac{1}{D_{\perp,0}^{(r)}} - \frac{1}{D_{\perp}^{(r)}}\left[\rho_r^*\varepsilon F_{\perp}^{(rr)}(\varepsilon^2) + \phi_s F_{\perp}^{(rs)}(\varepsilon;\gamma)\right], \quad \frac{1}{D_{\parallel}^{(r)}} = \frac{1}{D_{\parallel,0}^{(r)}} - \frac{1}{D_{\parallel}^{(r)}}\phi_s F_{\parallel}^{(rs)}(\varepsilon;\gamma)\,, \text{(A13)}$$

where $F_{\perp}^{(rs)}(\varepsilon;\gamma)$ and $F_{\parallel}^{(rs)}(\varepsilon;\gamma)$ are given as Eq. (3a) and (3b) in the main text.

Approximate expressions for Eqs. (3a) and (3b) can be derived in the limit of large aspect ratio and high dynamical anisotropy, $\gamma >> 1$ and $(1+\gamma)\varepsilon << 1$, conditions which imply $D_{\perp}^{(r)} / D_{\parallel}^{(r)} << 1/(1+\gamma)^2 \sim (2R/L)^2$. Since $\zeta_0 \sim (1+\gamma)\varepsilon << 1$, the Legendre functions $q_n(x)$ are given in the oblate form and satisfy $q_n(\zeta_0)/q_n'(\zeta_0) \sim q_n(0)/q_n'(0) + \mathcal{O}(\zeta_0)$, and it is straightforward to then show

$$c_{2n}\left(\frac{\gamma}{1+\gamma}\right) = \delta_{n,0} + \mathcal{O}(\gamma^{-1}), \quad c_{2n+1}\left(\frac{\gamma}{1+\gamma}\right) = \frac{1}{2\gamma^2} + \mathcal{O}(\gamma^{-3})\,. \qquad \text{(A14)}$$

Thus one has

$$\frac{D_{\perp}^{(r)}}{D_{\perp,0}^{(r)}} \sim 1 - \rho_r^* a_{\perp}^{(rr)}\varepsilon - \phi_s a_{\perp}^{(rs)}(1+\gamma)^2\varepsilon \sim 1 - \rho_r^* a_{\perp}^{(rr)}\varepsilon - \phi_s a_{\perp}^{(rs)}\gamma(1+\gamma)\varepsilon\,, \qquad \text{(A15a)}$$

$$\frac{D_{\parallel}^{(r)}}{D_{\parallel,0}^{(r)}} \sim 1 - \phi_s\left(\frac{1+\gamma}{\gamma}\right)^2 \frac{a_{\parallel}^{(rs)}}{\varepsilon} \sim 1 - \phi_s\,\frac{a_{\parallel}^{(rs)}}{\varepsilon}\,, \qquad \text{(A15b)}$$

where higher order terms in $(1+\gamma)\varepsilon$ and $1/\gamma$ have been neglected, and $a_{\perp}^{(rr)}$, $a_{\perp}^{(rs)}$, $a_{\parallel}^{(rs)}$ are numerical constants defined by

$$a_{\perp}^{(rr)} \equiv F_{\perp}^{(rr)}(0) = \frac{1}{3\sqrt{2\pi}}, \quad a_{\perp}^{(rs)} \equiv -\frac{3}{2} c_0(0) \frac{q_0(0)}{q_0'(0)} = 3\left(\frac{\pi}{4}\right)^2, \quad a_{\parallel}^{(rs)} \equiv -\frac{3}{2} \frac{q_1(0)}{q_1'(0)} = \frac{3}{\pi}. \quad \text{(A16)}$$

Solving Eq. (A15) for ϵ gives

$$\varepsilon \sim \frac{\alpha}{2}\left(\sqrt{1+\frac{4\varepsilon_0^2}{\alpha^2}}-1\right) \sim \frac{1}{2\alpha} \quad (\alpha >> 1), \quad \text{(A17)}$$

where

$$\alpha \equiv \left[a_{\perp}^{(rs)} \varepsilon_0^2 \gamma (1+\gamma) - a_{\parallel}^{(rs)} \right] \phi_s + \rho_r^* \varepsilon_0^2 a_{\perp}^{(rr)}. \quad \text{(A18)}$$

The opposite signs of the $a_{\perp}^{(rs)}$ and $a_{\parallel}^{(rs)}$ terms in Eq. (A18) reflect the competing effect of the two diffusivities on the diffusion anisotropy, but the latter contribution is $\mathcal{O}(\gamma^2)$ weaker than the former.

The renormalized reptation form of Eq. (4) is obtained by further assuming $\rho_r^* >> 1$ (or $\rho_r^* > 40$ in practice) where the pure rod fluid reptation regime is well-defined and the diffusion anisotropy and the tube diameter scale as $D_{\perp}^{(r)} / D_{\parallel}^{(r)} \sim 1/(\rho_r^* a_{\perp}^{(rr)})^2$ and $d_{T,0}/L \sim 16\sqrt{2}/(\pi \rho_r^*)$, respectively[2]. Applying these relations to Eq. (A18) and using Eq. (A16) yields

$$\frac{D_{\perp}^{(r)}}{D_{\parallel}^{(r)}} = \left(\frac{D_{\perp}^{(r)}}{D_{\parallel}^{(r)}}\right)_{\text{pure rods}} \left[1 + \frac{3}{4}\left(\frac{\pi^{3/2} a_{\perp}^{(rs)}}{4}\right) \frac{d_{T,0}}{2R}\left(1+\frac{L}{2R}\right)\phi_s\right]^{-2}, \quad \text{(A19a)}$$

which can be expressed as

$$\frac{D_{\perp}^{(r)}}{D_{\parallel}^{(r)}} = \left(\frac{D_{\perp}^{(r)}}{D_{\parallel}^{(r)}}\right)_{\text{pure rods}} \left[1 + (1.93)\phi_{\text{eff}}\right]^{-2} = \left(\frac{D_{\perp}^{(r)}}{D_{\parallel}^{(r)}}\right)_{\text{pure rods}} \left(\frac{d_T}{d_{T,0}}\right)^2, \quad \text{(A19b)}$$

where $d_T / d_{T,0} \sim [1+(1.93)\phi_{\rm eff}]^{-1}$ is the effective tube diameter in the composite[1]. Thus, Eq. (A18b) establishes the renormalized reptation law discussed in the main text.

B. Needle Localization Transition

Our numerical results for the needle dynamic localization transition are shown in Fig. S1. We first summarize and discuss our findings in physical terms.

As expected, the sphere critical volume fraction for needle localization, ϕ_c, always decreases with γ and ρ_r^*. However, all parameter dependences can be understood in a universal manner as follows. First, Fig. S1 shows that $\phi_{c,0} \equiv \phi_c(\rho_r^* = 0) \propto 1/\gamma$ for $\rho_r^* \to 0$ and $\gamma >> 1$. This implies needle localization occurs at a critical volume fraction of an "effective object" of sphero-cylindrical geometry with volume $\sim R^2 L$ (ala a rod-sphere "cross" virial coefficient), which can be interpreted as a needle surrounded by spheres in contact with it. Second, the effect of finite rod concentration enters only via a multiplicative factor, $\phi_c / \phi_{c,0}$, which is entirely controlled by $\rho_r^* / (1+\gamma)$, as shown in the inset of Fig. S1. At high aspect ratio, the latter quantity scales as $2R / d_{T,0}$ in the entangled regime, an intuitive ratio that characterizes the ability of spheres to "cap" the tube. Thus, dynamic localization in entangled needle liquids is understood as an extreme consequence of the blocked reptation effect.

Analytic derivations of the above results can be obtained by analyzing Eqns. (A15a) and (A15b). First, for the single-rod ($\rho_r^* \to 0$) case, equating both diffusivities in Eq. (A15a) and (A15b) to zero readily provides $\phi_{c,0} \equiv \phi_c(\rho_r^* = 0) = 4/[3\sqrt{\pi\gamma(1+\gamma)}] \sim 4/(3\sqrt{\pi})\gamma^{-1}$. Such simple scaling relations are not generally available for finite ρ_r^*, but its parameter dependence can be determined by using the above form of $\phi_{c,0}$ to express Eqs. (A15a) and (A15b) in terms of $\phi_c / \phi_{c,0}$. This readily leads to

$$0 = 1 - \frac{\rho_r^*}{1+\gamma}\sqrt{\frac{a_\perp}{a_\parallel}}\left(\frac{\varepsilon_c}{\varepsilon_{c,0}}\right)F_\perp^{(rr)}(\varepsilon_c^2) - \left(\frac{\phi_c}{\phi_{c,0}}\right)\left(\frac{\varepsilon_c}{\varepsilon_{c,0}}\right), \quad 0 = 1 - \left(\frac{\phi_c}{\phi_{c,0}}\right)\left(\frac{\varepsilon_{c,0}}{\varepsilon_c}\right), \qquad \text{(A20)}$$

where $\varepsilon_c \equiv \varepsilon(\phi_s = \phi_c)$ and $\varepsilon_{c,0}$ represents its single-rod limit. Equation (A20) indicates that $\phi_c / \phi_{c,0}$ is a function of $\rho_r^* / (1+\gamma)$, which provides theoretical support for the essentially perfect collapse seen in the inset of Fig. S1. Also, one generally obtains $\varepsilon_c = \phi_c / a_\parallel^{(rs)}$ from Eq. (A15b), leading to $D_\perp^{(r)} / D_\parallel^{(r)} \propto \phi_c^2$ at localization.

References

(1) Yamamoto, U.; Schweizer, K. S. ACS Macro Lett., **2013**, *2*, 955-959.

(2) Szamel, G. Phys. Rev. Lett., **1993**, *70*, 3744-3747; Szamel, G.; Schweizer, K.S. J. Chem. Phys., **1994**, *100*, 3127-3141.

(3) Lamb, H. *Hydrodynamics*; Dover: New York, 1945.

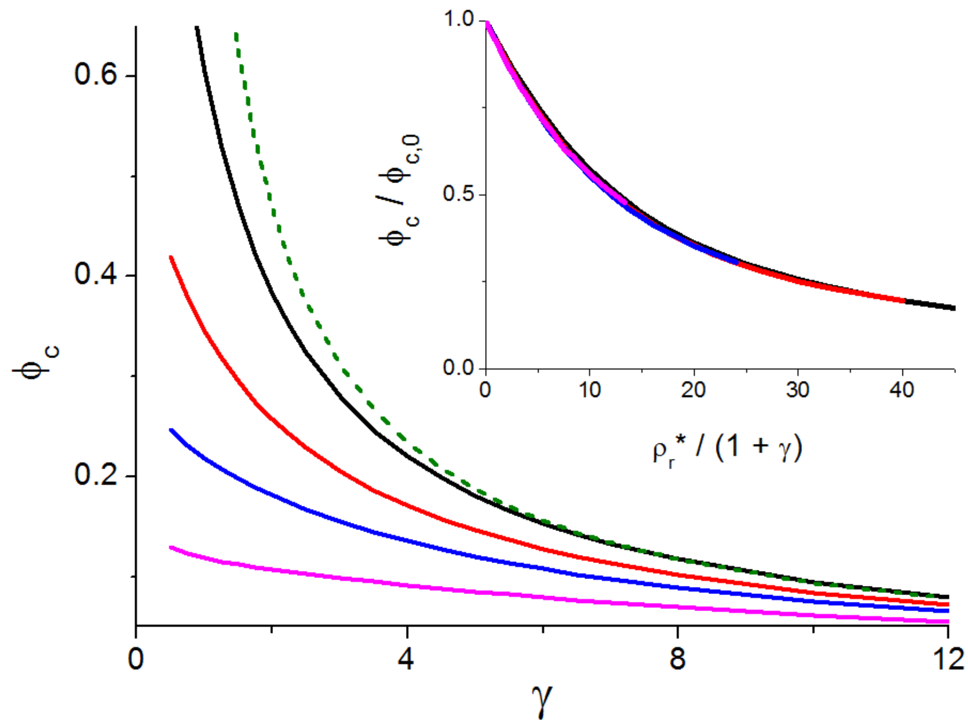

FIG. S1: Critical rod localization volume fraction as a function of aspect ratio for $\rho_r^* =$ 0 (black), 20 (red), 40 (blue), 80 (pink). The green dashed curve shows the asymptotic result in the dilute single rod limit where $\phi_c \propto 1/\gamma$ for $\gamma >> 1$. (Inset) Master plot. Ratio of the critical volume fraction relative to the dilute rod limit value as a function of rod number density divided by $1+\gamma$. Each curve corresponds to $\gamma =$ 1 (black), 2 (red), 4 (blue) and 8 (pink).